Supporting Information

Self-assembled composite microparticles with surface protrudent porphyrin nanoparticles enhance cellular uptake and photodynamic therapy

Wenbo Zhang [a], Huiying Li [a], Ying Qin [a] and Changyou Gao [a,b] *

[a] *MOE Key Laboratory of Macromolecular Synthesis and Functionalization, Department of Polymer Science and Engineering, Zhejiang University, Hangzhou 310027, China*

[b] *Dr. Li Dak Sum & Yip Yio Chin Center for Stem Cell and Regenerative Medicine, Zhejiang University*

**Corresponding author: cygao@mail.hz.zj.cn*

Materials

Poly(allylamine hydrochloride, PAH, 120-200 kDa) was purchased from Alfa Aesar. Fluorescein isothiocyanate (FITC), oregon green isothiocyanate (OGITC), rhodamine B isothiocyanate (RBITC), 3-(4,5-dimethylthiazol-2-yl)-2,5-diphenyltetrazolium bromide (MTT), 4,6-diamidino-2-phenylindole dihydrochloride (DAPI), 9, 10-anthracenediyl-bis(methylene)dimalonic acid (ABDA) and other chemicals were purchased from Sigma-Aldrich. Lyso Tracker®Red was purchased from Invitrogen. Calcium nitrate terahydrate, sodium carbonate, ethylenediamine tetraacetic acid (EDTA), glutaraldehyde (GA, 25%), HCl solution (10 mol L^{-1}), and other organic solvents were purchased from Sinopharm Chemical Reagent Company (Beijing, China). GA solution (25%) and HCl solution (10 mol/L) were diluted to the desired concentrations. Tetrahydrofuran (THF) and methanol were purified by distillation after treatment with calcium hydride and magnesium ribbons, respectively. Other chemicals were used as received. The water used in all experiments was prepared using a Millipore Milli-Q purification system.

Preparation of the micro-nanoparticles

1. Fabrication of PAH-g-Por microparticles (MPs)

The PAH-g-Por MPs were fabricated by taking advantage of the Schiff base reaction between PAH doped in $CaCO_3$ microparticles and 2-formyl-5,10,15,20-tetraphenylporphyrin (Por-CHO). After removing the templates and crosslinking with GA, PAH-g-Por MPs were obtained.

Por-CHO was synthesized according to the method reported previously (Scheme S1), [1, 2] and its chemical structure was verified by ^{1}H NMR and mass spectrum. Porous spherical $CaCO_3$ microparticles doped with PAH ($CaCO_3$ (PAH)) were prepared by mixing $Ca(NO_3)_2$ solution containing PAH and $NaCO_3$ solution, and their morphology and PAH content were characterized by SEM and thermal gravimetric analysis. [3]

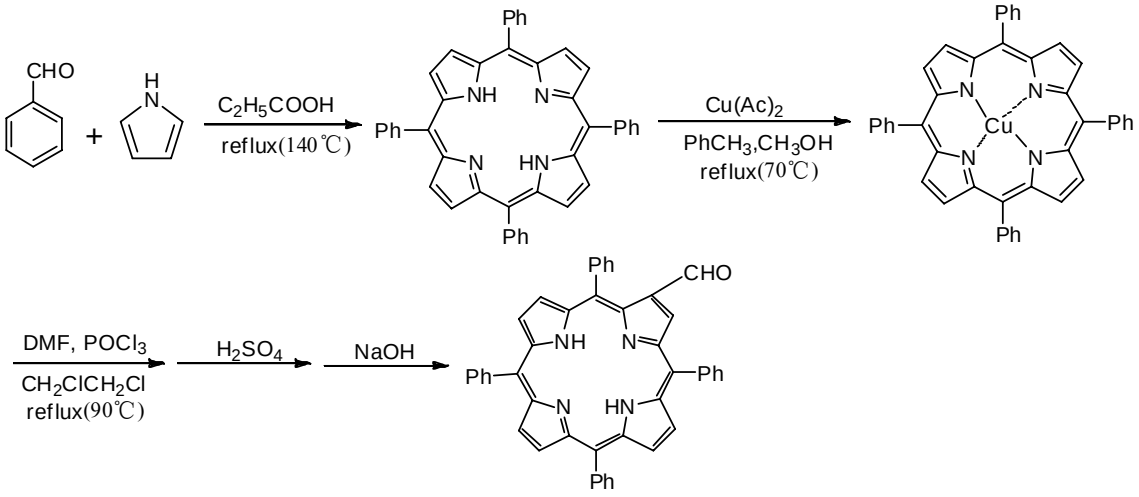

Scheme S1 Synthesis of Por-CHO.

5 mL $CaCO_3$ (PAH) microparticles (20 mg/mL in methanol) were added into 5 mL Por-CHO/ THF solution (1 mg/ mL). The mixture was allowed to react in a sealed container at 30 ^{o}C for 3 d. The obtained $CaCO_3$ (PAH-g-Por) microparticles were washed with THF several times to remove the excess Por-CHO. After being washed with water to replace the THF, the $CaCO_3$ (PAH-g-Por) microparticles were incubated in 50 mL EDTA solution (0.2 M, pH 7.0) overnight to remove the sacrificial $CaCO_3$ templates. Then the obtained PAH-g-Por microparticles were washed with water three times using a membrane filter (membrane pore size: 0.45 μm). Thereafter, the microparticles were crosslinked in 50 mL GA solution (0.33%) at 30 ^{o}C. After 10 h, the microparticles were washed with water to obtain PAH-g-Por MPs.

2. Preparation of PAH-g-Por micro-nanoparticles (MP-NPs)

50 mL pH 1 HCl solution was added to 5 mL PAH-g-Por MPs (5×10^8/mL in water), which was then incubated at 30 ^{o}C for 1 h. The HCl solution was removed by centrifugation, and the obtained MP-NPs were dispersed in 50 mL water after washed with water.

To monitor the formation process of NPs on the MPs, one portion of the solution was taken out during the incubation at desired time intervals, which was washed with water after removal of HCl

solution.

3. Fluorescence-labeling of MP-NPs and MPs

0.5 mL MP-NPs or MPs (5×10^8/mL in water) was added into 5 mL $NaHCO_3/Na_2CO_3$ buffer (0.1 M/0.1 M, pH 9.5). Then 15 μL OGITC or 20 μL RBITC (1 mg/mL stock solution in DMSO) was added. The mixture was maintained at room temperature overnight in dark. Then the mixture was centrifuged (5000 rpm, 2 min) to remove the supernatant, and the particles were washed with $NaHCO_3/Na_2CO_3$ buffer and water three times successively to remove the excess dyes, respectively.

4. Test of colloidal stability of MP-NPs and MPs

The colloidal stability of MP-NPs and MPs in phosphate buffered saline (PBS) and cell culture medium containing fetal bovine serum (FBS) was tested in terms of photos and hydrodynamic diameter. The particles were dispersed in cell culture medium containing 10% FBS and 50% FBS, PBS and water at a concentration of 1×10^7/ml. The appearance status of these dispersion systems was recorded with a digital camera and hydrodynamic diameter of the particles was measured with a dynamic light scattering (DLS) instrument. Then the dispersion systems were incubated at 37 ^oC overnight. After re-dispersing the particle precipitation, the appearance status recording and the hydrodynamic diameter measurement were performed again, respectively. The results before and after incubation were compared to indicate the stability of the particles.

In order to further verify colloidal stability of the particles, the medium was removed by centrifugation (10000 rmp, 2min) and the particles were dispersed in water (1×10^7/ml) to measure the hydrodynamic diameter again.

5. Detection of singlet oxygen ($^1O_2$) generation of MP-NPs in solution

The $^1O_2$ generation of MP-NPs or MPs in solution was detected by using ABDA as the $^1O_2$ sensor. ABDA can react with $^1O_2$ to form the corresponding endoperoxide, resulting in its absorption decrease at 378 nm. MP-NPs or MPs (final concentration 2×10^6/mL) were mixed with ABDA (final concentration 100 μM) in water. The ABDA solution, MP-NPs suspension and MPs suspension in water, which had the same concentrations mentioned above, were used as control samples, respectively. The sample solutions were added into a 96-well plate (50 μL/ well) and were irradiated with 445 nm laser source (light density 0.3 W/cm^2). After each irradiation for 10 s, the absorbance at 378 nm was measured with a microplate reader (M200 Pro, Tecan). The experiment was performed in total 60 s.

6. Characterizations of materials and particles

The **^{1}H nuclear magnetic resonance (^{1}HNMR)** spectrum was recorded on a Bruker DMX500, by using $CDCl_3$ as the solvent. The **mass spectrum (MS)** was obtained from a Bruker Esquire 3000plus ion trap mass spectrometer (Brucker-Franzen Analytik GmbH, Bremen, Germany): nitrogen was used as nebulizing gas at a pressure of 10 psi and drying gas at a flow rate of 5 L min^{-1}. The drying gas temperature was set at 250 °C and the capillary voltage was set at 4000 V. The solution was infused to the mass spectrometer with a syringe pump at a flow rate of 6 μL min^{-1}. **Scanning electron microscopy (SEM):** A drop of the sample suspension was placed onto a clean glass, and dried naturally. The samples were sputtered with gold, and were observed with a Hitachi S-4800 SEM at an acceleration voltage of 3 kV. **Confocal laser scanning microscopy (CLSM):** The particle suspensions were placed onto clean glass slides, and were observed with a Leica TCS SP5 system (100× oil immersion using commercial software). **Fourier transform infrared (FTIR) spectra** were recorded on a Bruker Equinox 55/S instrument using KBr pellets. **Elemental analysis** was measured on a Vario MICRO cube instrument from Elementar Analysensysteme GmbH. The samples for FTIR and elemental analysis were obtained by freeze-drying. The **ultraviolet-visible (UV–Vis) absorption spectra** were recorded with a Shimadzu UV2550 spectrophotometer. **Fluorescence emission spectra** were recorded with a Shimadzu RF-5301PC instrument (excitation wavelength: 420 nm). **Zeta potential/size** was measured on a zeta potential/submicron size analyzer (Delsa TM Nano (Beckman Coulter) at room temperature (25 ^oC). Each value was averaged from three parallel measurements. For UV-Vis, fluorescence and zeta potential/size measurements, the sample solutions were used directly.

Cell experiments

1. Cell culture

The human lung adenocarcinoma epithelial cells (A549 cells), human liver hepatocellular carcinoma cells (HepG2 cells), murine macrophage cells (RAW 264.7 cells) and mouse embryo fibroblast cell line (NIH3T3 cells) were purchased from the Cell Bank of Typical Culture Collection of the Chinese Academy of Sciences (Shanghai, China). Primary human normal hepatocytes (Hepli cells) were obtained from the First Affiliated Hospital, College of Medicine, Zhejiang University. The A549 cells were cultured in RPMI-1640 medium (Gibco, USA). The HepG2, RAW 264.7, and NIH3T3 cells were cultured in high-glucose Dulbecco's modified eagle medium (DMEM) (Gibco, USA). The Hepli cells were cultured in low-glucose DMEM (Gibco, USA). The medium was supplemented with 5%

FBS (Gibco), 100 U/mL penicillin and 100 μg/mL streptomycin. The cells were incubated in an incubator at 37 °C supplied with 5% CO_2 and 100% humidity.

2. Cellular uptake of MP-NPs and MPs

Cellular uptake kinetics

The A549 or HepG2 cells were seeded at a density of 1×10^5 cells per well on 24-well plates, and were allowed to attach for 24 h. Then 2×10^6 OGITC-labelled MP-NPs or OGITC-labelled MPs dispersed in 1 mL medium were added to each well (particles: cells = 20:1). The cells and particles were co-incubated for different time. After being washed with PBS three times to remove the free particles, the cells were detached with trypsinization and dispersed in PBS at a concentration of about 1.6×10^5/mL. The average fluorescence intensity per cell and the ratio of cells with fluorescence was measured with flow cytometry (FACS Calibur, BD).

Cellular uptake performance

The difference of cellular uptake performance of MP-NPs and MPs was analyzed with flow cytometry and CLSM. For the flow cytometry measurements, A549, HepG2, Hepli, RAW 264.7 or NIH3T3 cells were incubated with OGITC-labelled MP-NPs or OGITC-labelled MPs at a particle-to-cell ratio of 20:1 for 3 h. The cell culture conditions, processing procedures after co-incubation, and the measurement method were same as above.

For the CLSM measurements, the A549, HepG2 or Hepli cells were seeded at a density of 8×10^4 on a 20-mm cell culture dish with a glass bottom, and were cultured for 24 h. Then the cells were incubated with OGITC-labelled MP-NPs or OGITC-labelled MPs at a particle-to-cell ratio of 20:1 for 3 h. After being washed with PBS three times to remove the free particles, the cells were fixed with 4% paraformaldehyde/PBS at 37 ^oC overnight. Then the cells were treated with Triton X-100 in PBS (0.5% v/v) at 37 ^oC for 10 min to increase the permeability of cell membrane. After being incubated in BSA/PBS solution (5% w/w) at 37 ^oC for 2 h to block nonspecific adsorption, the cells were stained with DAPI (2 μg/mL) for 2 h at 37 ^oC in dark. Images were acquired by a Leica TCS SP5 CLSM (63×/1.4 NA oil immersion objective using commercial software). DAPI, OGITC and porphyrin were excited at 408, 488 and 543 nm, respectively.

Competitive cellular uptake of MP-NPs and MPs

The competitive cellular uptake of MP-NPs and MPs was analyzed with a microplate reader and CLSM. For quantitative analysis of internalization number of MP-NPs and MPs co-incubated with

cells simultaneously, the A549 or HepG2 cells were incubated with OGITC-labelled MP-NPs and RBITC-labelled MPs at a (MP-NPs)/ MPs/ cell ratio of 10/10/1 for 3 h. After being washed with PBS three times to remove the free particles, the cells were detached with trypsinization and dispersed in PBS at a concentration of about 1.6×10^5/ mL. Meanwhile, OGITC-labelled MP-NPs and RBITC-labelled MPs were suspended in PBS at a concentration of 3.2×10^6/ mL. The fluorescence intensity of OGITC and RBITC in the cell and particle suspensions was measured in a black 96-well plate with a microplate reader (M200 Pro, Tecan). The excitation and emission wavelengths were set at 488 nm and 530 nm for OGITC, and 543 nm and 580 nm for RBITC, respectively. To determine the average internalization number of MP-NPs and MPs, the fluorescence intensity of suspended cells and particles was compared.

For the CLSM measurements, the A549 or HepG2 cells were seeded at a density of 8×10^4 on a 20-mm cell culture dish with a glass bottom and were cultured for 24 h. Then the cells were co-incubated with OGITC-labelled MP-NPs and RBITC-labelled MPs at a MPs/(MP-NPs)/cell ratio of 10/10/1. After co-incubation, the samples were treated and measured with the same procedures as the separate cellular uptake performance experiments mentioned above.

Track the internalization process of MP-NPs and MPs

The internalization process of MP-NPs and MPs were tracked with CLSM, SEM and in situ time-lapse microscopy. For the CLSM measurements, the A549 or HepG2 cells were seeded at a density of 8×10^4 on a 20-mm cell culture dish with a glass bottom, and were cultured for 24 h. Then the cells were incubated with MP-NPs or MPs at a particle-to-cell ratio of 20:1 for 1 h, 3 h and 6h, respectively. After co-incubation, the samples were treated with the same procedures as the above cellular uptake experiments with CLSM mentioned above. Then the samples were characterized with a Zeiss LSM 780 CLSM (40×/1.4 NA oil immersion objective using commercial software). DAPI, OGITC and porphyrin were excited at 405, 488 and 561 nm, respectively.

For the in-situ monitoring with time-lapse microscopy, the A549 or HepG2 cells were seeded at a density of 6×10^4 on a 20-mm cell culture dish with a glass bottom, and were cultured for 24 h. Then the cells were incubated with MP-NPs or MPs at a particle-to-cell ratio of 20:1 and were recorded in situ for 3 h (bright field; time interval, 2 min) with a time-lapse microscope (Leica DMI6000B) equipped with a cell culture chamber (37 °C and 5% CO_2 humidified atmosphere).

For the SEM measurements, a sterilized glass slide was placed into a well of a 48-well cell culture

plate. A549 or HepG2 cells were seeded in the wells with a density of 2×10^4 per well and were cultured for 24 h. Then the cells were incubated with MP-NPs or MPs at a particle-to-cell ratio of 20:1 for 1 h, 3 h and 6h, respectively. After being washed with PBS three times to remove the free particles, the cells were fixed with 4% paraformaldehyde/PBS at 37 ^{o}C overnight. Then the samples were washed with fresh PBS and were dehydrated with ethanol aqueous solution of increasing gradient concentrations (5, 10, 20, 30, 50, 80, and 100%) for 15 min, respectively. After dehydration, the samples were dried by critical point drying. The obtained samples were sputtered with gold and were characterized with a Hitachi SU8010 SEM at an operation voltage of 3 kV.

Intracellular distribution of MP-NPs and MPs

Fluorescent staining of lysosomes was performed to display the intracellular distribution of MP-NPs and MPs. A549 cells were seeded at a density of 6×10^4 on a 20-mm cell culture dish with a glass bottom, and were cultured for 24 h. Then the cells were incubated with OGITC-labelled MP-NPs or MPs at a particle-to-cell ratio of 20:1 for 3 h. After co-incubation, the cells were washed with PBS three times to remove free particles, and then Lyso Tracker®Red was added (1 μM). The cells were cultured in dark for 30 min. After removal of cell culture medium, the cells were washed with PBS three times and observed with CLSM. OGITC and Lyso Tracker®Red were excited at 488 and 561 nm, respectively.

3. Photodynamic therapy studies

Cell activity assay

Cell activity was determined with MTT assay as an indicator of cell damage or cytotoxicity. A549 or HepG2 cells were seeded at a density of 1×10^4 cells per well on 96-well plates and were incubated for 24 h. Then the cells were incubated with MP-NPs or MPs at a particle to cell ratio of 20: 1 for 3 h, followed by washing three times with PBS to remove the free particles. Thereafter, 50 μL medium without phenol red indicator and FBS was added to each well, and the cells were irradiated with 445 nm laser source for 5 min at a power density of 0.3 W/cm^2. After irradiation, the cells were further cultured for 12 h, and were then washed with PBS twice. 100 μL of cell culture medium without phenol red indicator and 20 μL MTT/PBS solution (5 mg/mL) were added into each well. After 3.5 h incubation at 37 ^{o}C, the MTT medium solution was removed carefully, and 100 μL dimethyl sulfoxide (DMSO) was added into each well to dissolve the purple formazan crystals generated by the mitochondria dehydrogenase. After incubation at 37 ^{o}C for 15 min, 50 μL formazan/DMSO solution

was pipetted into a well of another new 96-well plate. The absorbance at 490 nm was measured by a microplate reader (M200 Pro, Tecan). Cell activity was expressed as the ratio of absorbance of the experimental groups to that of the control group in which the cells were incubated with cell culture medium only. Data were expressed as average ± SD (n = 5). To measure the dark cytotoxicity of the particles and influence of light irradiation on photo-cytotoxicity, cells incubated with MP-NPs or MPs only, and cells with light irradiation only were set as the control groups at the same time. Meanwhile, the influence of particle-to-cell ratio and light fluence on the PDT effect was studied with A549 cells by the same method.

Intracellular ROS detection

The intracellular ROS generation of cells upon light irradiation was detected with the dichlorofluorescein diacetate (DCFH-DA) cellular reactive oxygen species assay kit (Beyotime, China). A549 and HepG2 cells were seeded at a density of 2×10^4 and 1×10^4 cells per well on 96-well plates, and were cultured for 24 h, respectively. The MP-NPs or MPs were then added to each well at a particle-to-cell ratio of 20:1, and were incubated with cells for 3 h. The cells were then washed three times with PBS to remove the free particles. 50 μL medium without phenol red indicator and FBS was added to each well, and the cells were irradiated with 445 nm laser source for 5 s (fluence: 0.3 W/cm^2). The cells incubated with MP-NPs or MPs only without light irradiation and the cells irradiated with light only were set as the control groups. The cells treated with Rosup agent in culture medium (0.2 mg/mL) for 20 min and the untreated cells were set as the positive and negative control groups, respectively. Then the medium was replaced by 50 μL serum and phenol red free medium containing 2×10^{-6} M DCFH-DA. After incubation at 37 ^{o}C for 30 min in dark, the cells were carefully washed with serum free medium three times to remove excess DCFH-DA. The fluorescence images were recorded with the 10×objective on a fluorescence microscope (IX81, Olympus, Japan). The excitation wavelength was 488 nm. The intensity of obtained images was further analyzed by Image J software.

Statistical analysis

Data are expressed as mean ± standard deviation (SD). Statistical analysis was determined by one-way analysis of variance (ANOVA) with the Origin software. Means comparison was performed with the Tukey's method. A p value < 0.05 is considered statistically significant.

Results

1. Fabrication of MPs

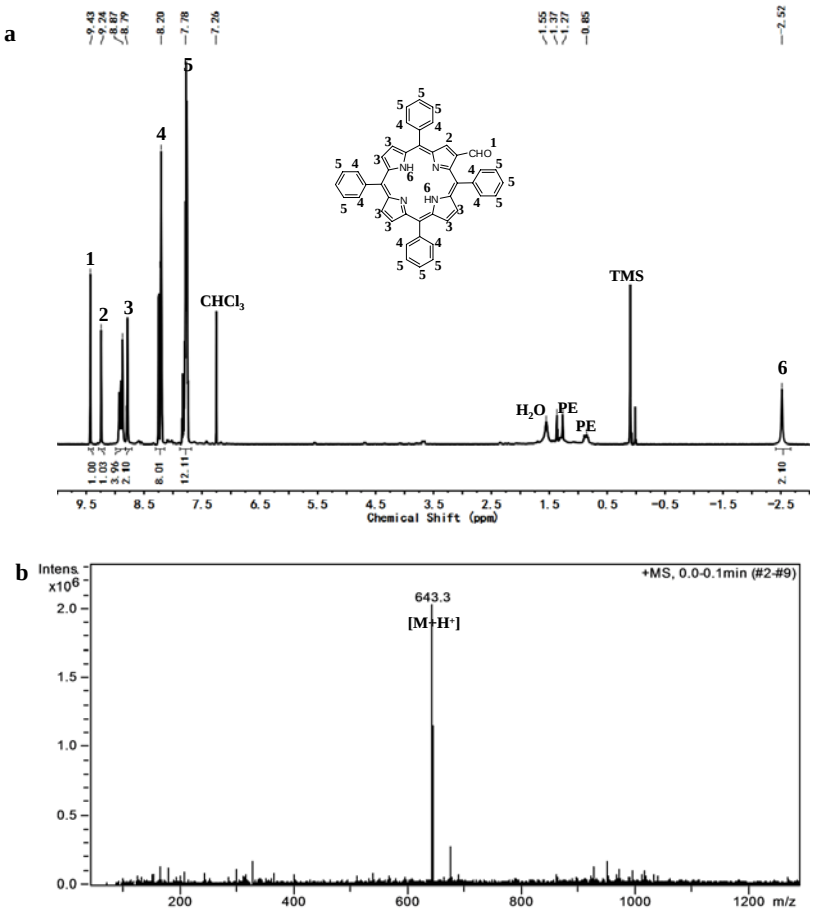

Figure S1 (a) ^{1}H-NMR spectrum of Por-CHO in $CDCl_3$ (PE= petroleum ether). (b) Mass spectrum (ESI) of Por-CHO.

The chemical structure of Por-CHO was verified by ^{1}H NMR and mass spectrum. ^{1}H NMR (500 MHz, $CDCl_3$; Figure S1a): δ = −2.52 (br s, 2H, inner NH), 7.74−7.85 (m, 12H, m- and p-PhH), 8.19−8.25 (m, 8H, o-PhH), 8.78−8.80 (m, 2H, β-pyrrolic H), 8.86−8.94 (m, 4H,β-pyrrolic H), 9.24 (br s, 1H, H-3), 9.43 (s, 1H, CHO). MS (ESI) ($C_{45}H_{30}N_4O$, exact mass = 642.8): calcd m/z for [M + H^+], 643.8; found, 643.3 (Figure S1b).

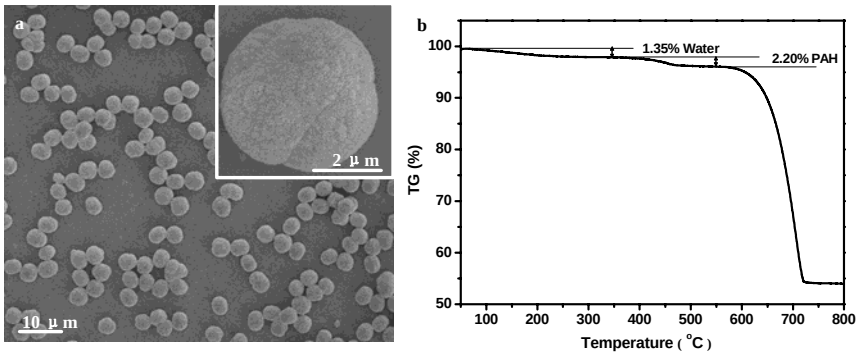

Figure S2 (a) SEM image of PAH-doped $CaCO_3$ particles (inset, higher magnification). (b) Thermogravimetric analysis curve of PAH-doped $CaCO_3$ particles (20 ^{o}C/ min heating rate in nitrogen).

2. Preparation of MP-NPs

Table S1 Size and zeta potential of MP-NPs and MPs in water

	MP-NPs	**MPs**
Size (μm)	1.84	1.71
Zeta potential (mV)	30.3	33.6

The colloidal stability of MP-NPs and MPs in PBS and cell culture medium containing FBS was characterized by direct observation and DLS.

After the influence of proteins (<200 nm) in cell culture medium containing FBS was deducted, the hydrodynamic diameters of particles in the medium was changed in a very small range after incubation at 37 ^{o}C overnight (Table S2), suggesting the good stability of the dispersion systems. Moreover, when the particles were re-dispersed in water, their size was similar to that of the untreated particles in water too (Table S3). In situ microscopy images showed that after incubation in the medium (10% FBS) for three days, the particles were still very dispersive and intact (Figure S4a-d). These results indicate the good stability and dispersibility of the particles in medium, so that no obvious aggregation or disruption occurs.

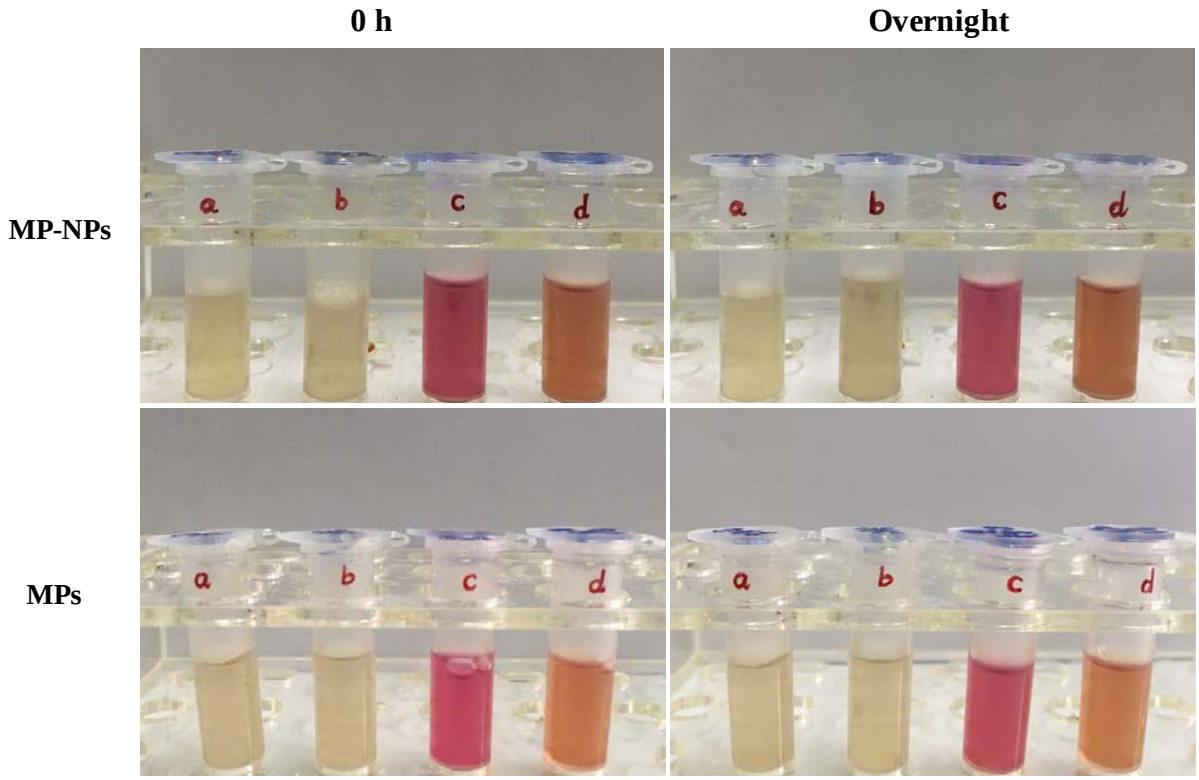

Figure S3 Photos of MP-NPs and MPs before and after incubation in water (a), PBS (b), DMEM containing 10% FBS (c) and DMEM containing 50% FBS (d) overnight.

Table S2 Hydrodynamic diameter (nm) of MP-NPs and MP s under various conditions

	0 h				Overnight			
Sample	**Water**	**PBS**	**DMEM /10%FBS**	**DMEM /50%FBS**	**Water**	**PBS**	**DMEM /10%FBS**	**DMEM /50%FBS**
MP-NPs	1864±145	1918±185	1923±134	1937±162	1887±164	1986±185	1968±156	1972±139
MPs	1759±161	1823±173	1819±149	1836±134	1792±152	1875±166	1866±127	1873±152

Table S3 Hydrodynamic diameter (nm) of MP-NPs and MPs after co-incubated in DMEM containing FBS and re-dispersed in water

	0 h		Overnight	
Sample	**DMEM /10%FBS**	**DMEM /50%FBS**	**DMEM /10%FBS**	**DMEM /50%FBS**

MP-NPs	1918±158	1895±171	1925±147	1935±166
MPs	1803±142	1814±136	1811±155	1821±152

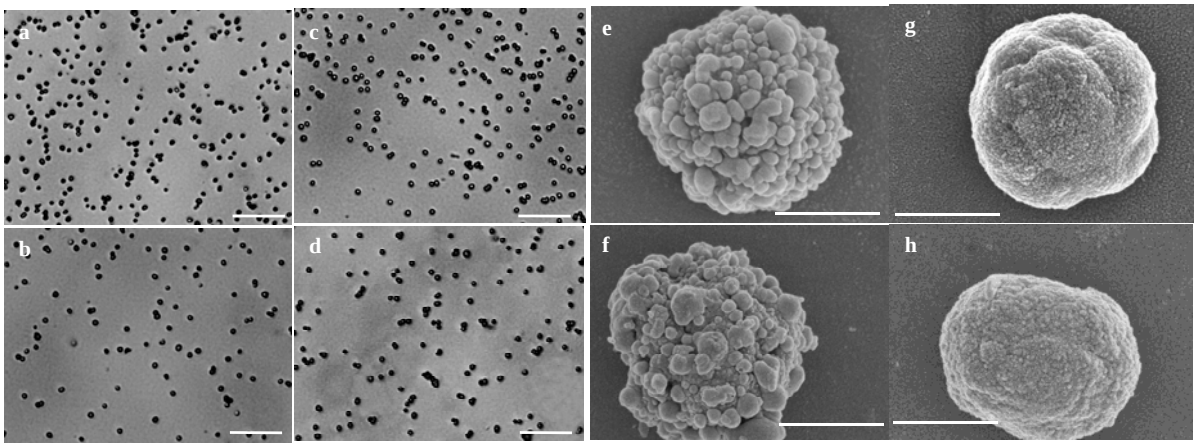

Figure S4 Optical microscopy (a-d) and SEM (e-h) images of MP-NPs (a, b, e, f) and MPs (c, d, g, h) before (a, c, e, g) and after (b, d, f, h) incubation in cell culture medium containing 10% fetal bovine serum for 3 d. In (a, c) and (b, d), the particles were dispersed in water and medium, respectively. The particles in (e) and (g) had been incubated in water for 3 d before measurement. Scale bars in (a-d) and (e-h) are 20 μm and 1 μm, respectively.

3. Composition analysis of MP-NPs and MPs

The bulk chemical compositions of the particles were analyzed with FTIR spectra (Figure S5). For the MPs, the appearance of the peak at 1636 cm^{-1} instead of the aldehyde group at 1668 cm^{-1} proves the formation of Schiff base bond by conjugation of porphyrin to PAH. The peak at 3420 cm^{-1} ($-NH_2$) and peaks at 2927 cm^{-1}, 2856 cm^{-1} and 1475 cm^{-1} ($-CH_2-$) indicate the presence of PAH. The peak at 3420 cm^{-1} (-NH-) and the peak at 3035 cm^{-1} (=CH) demonstrate the existence of porphyrin. The substitution degree of porphyrin on PAH in MPs was 12.3%, according to the elemental analysis result, and the corresponding loading efficiency of porphyrin was 47% (w/w) (Table S5). For the MP-NPs, the hydrolysis of C=N in the MPs at pH 1 was expected to result in Por-CHO formation. However, the aldehyde group peak of Por-CHO at 1668 cm^{-1} is not shown directly in the FTIR spectrum, due to the overlapping with the Schiff bond peak at 1631 cm^{-1} and the low absolute amount (Figure S5). Elemental analysis revealed that the molar ratio of porphyrin to PAH repeat units ([PAH]) in MP-NPs was 19.9% (Table S4), which corresponds to 57% loading efficiency (w/w), being among the

high-loading PDT photosensitizer delivery systems. [4, 5]

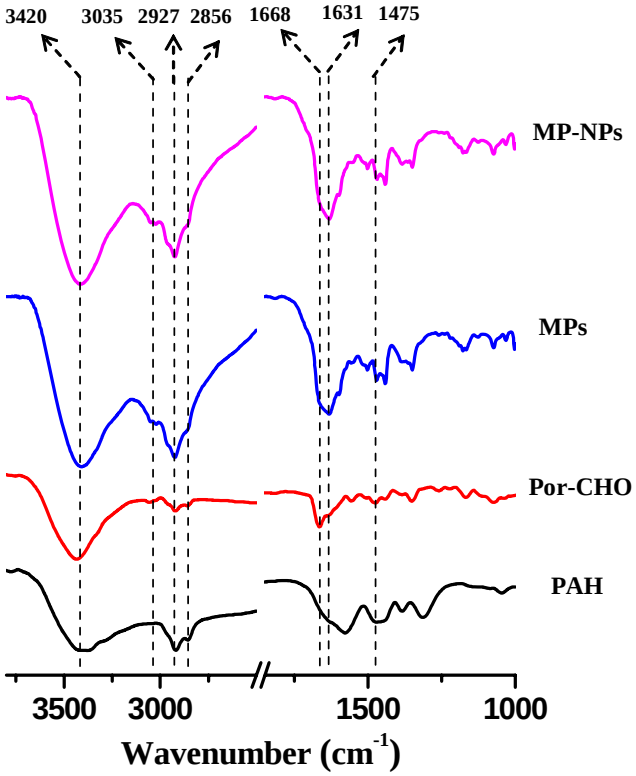

Figure S5 FTIR spectra of MP-NPs, MPs, Por-CHO and PAH.

Table S4 Loading ratio of porphyrin calculated based on the elemental analysis results

	MP-NPs	**MPs**
C/N (w/w)	6.61	5.99
porphyrin /[PAH] (%, n/n)	19.9	12.3
Loading ratio of porphyrin (%, w/w)	57	47

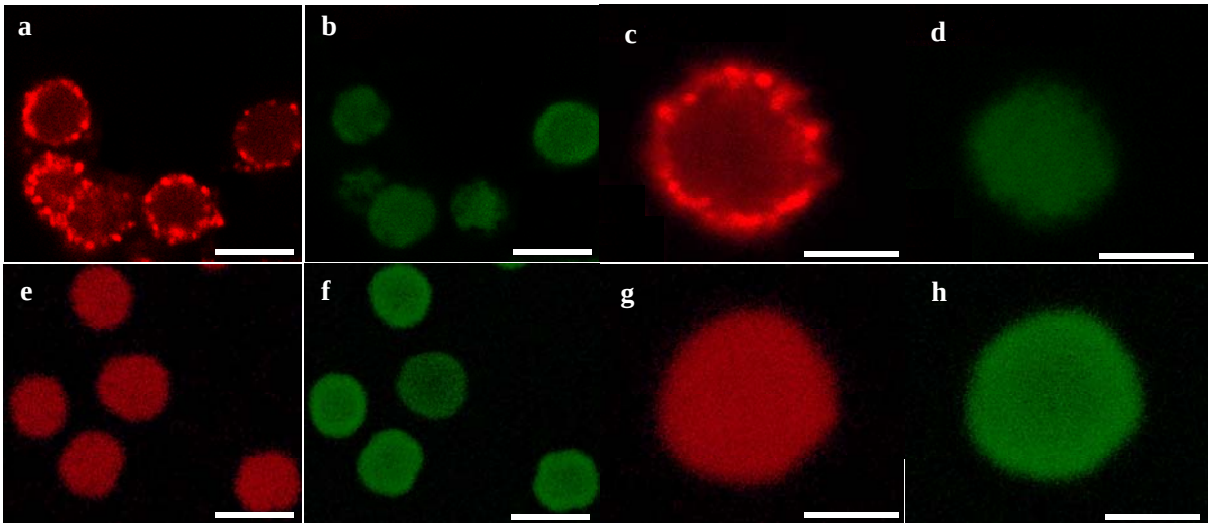

Figure S6 CLSM images of MP-NPs (a-d) and MPs (e-h) being prepared by using larger $CaCO_3$ as template. The red (a, c, e, g) and green (b, d, f, h) fluorescence represent the emission of porphyrin and FITC-PAH, respectively. Scale bar in (a, b, e, f) is 5 μm; scale bar in (c, d, g, h) is 2.5 μm.

4. Optical property analysis of MP-NPs and MPs

UV-Vis spectra were used to investigate the interacting features of porphyrin with neighboring molecules or moieties in the MP-NPs and MPs (Figure 2i). The MP-NPs presented the typical characteristics of free base porphyrin with a relatively strong Soret band centered at 435 nm and four weaker Q bands from 500 to 700 nm. The broadened and red-shifted Soret band indicates the porphyrin self-assembly in the form of J-aggregates, while the shoulder band around 420 nm can be attributed to the non-assembled porphyrin that is linked on PAH backbone or free. For the MPs, the Soret band is much weaker with higher degree of broadening and red-shift, suggesting stronger hydrophobic and π−π interactions in bigger aggregates. [6, 7]

5. Cellular uptake performance

The cellular uptake performance of the particles was tested in three kinds of normal cells as well to investigate whether this phenomenon has general applicability. For the Hepli normal liver cells and NIH3T3 fibroblast cells, the enhancement degree of both cellular uptake amount and ratio of MP-NPs was comparable to the situation for the A549 cells, which was around 2-fold (Figures S8, S9). For the RAW 264.7 macrophage cells, the enhancement degree was about 1.5-fold (Figure S9).

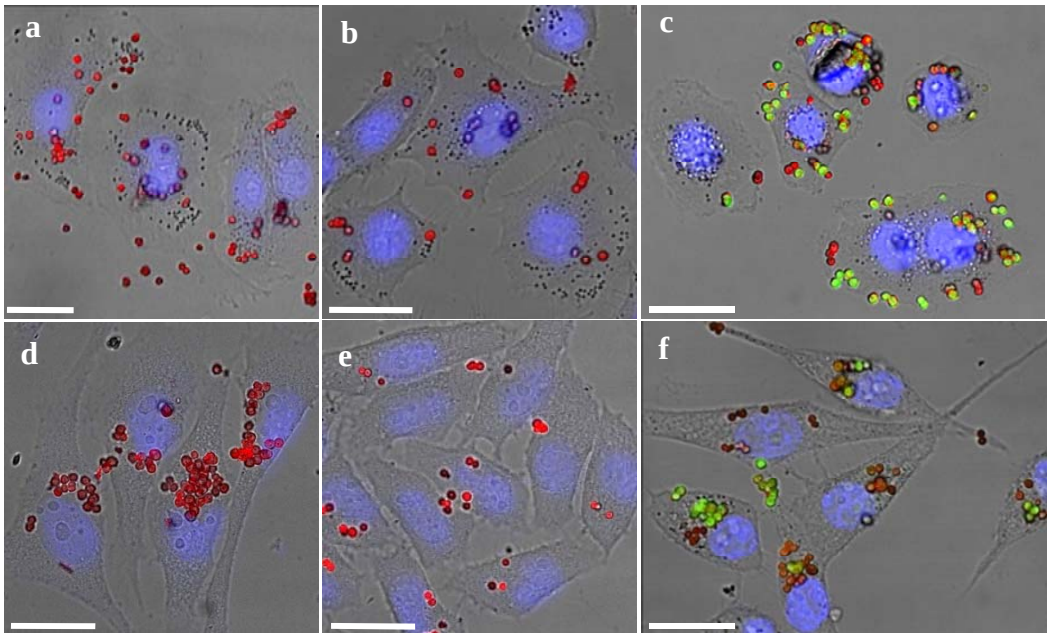

Figure S7 (a, b, d, e) CLSM images show the cellular uptake of MP-NPs (a, d) and MPs (b, e) after A549 (a, b) and HepG2 (d, e) cells were incubated with the particles at a particle-to-cell ratio of 20: 1 for 3 h. (c, f) CLSM images show the competitive uptake between OGITC-labeled MP-NPs (green) and RBITC-labeled MPs (red) after co-incubation with A549 (c) and HepG2 (f) cells at a ratio of 10:10:1 (MP-NPs: MPs: cells) for 3 h. Scale bar is 25 μm.

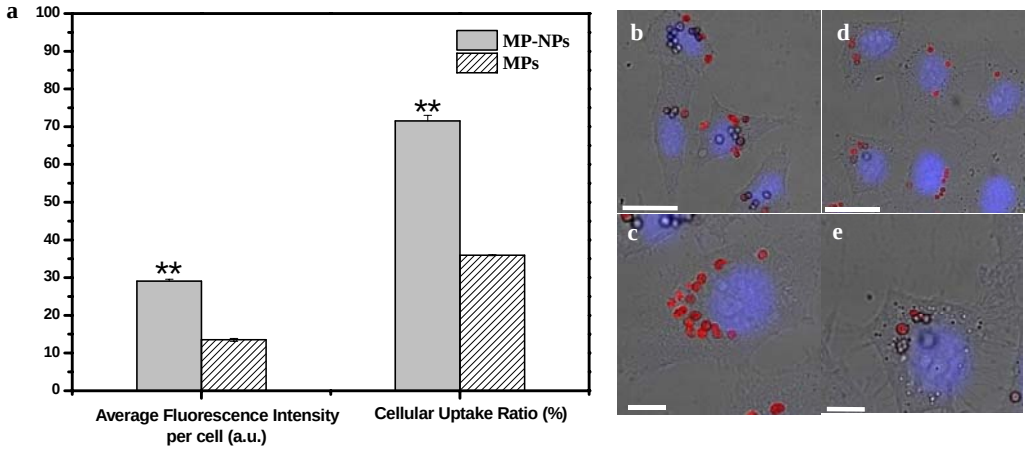

Figure S8 (a) Flow cytometry results show the cellular uptake amount and ratio of MP-NPs and MPs in Hepli cells (normal hepatocytes). (b-e) CLSM images show the cellular uptake performance of MP-NPs (b, c) and MPs (d, e). The particles were incubated with Hepli cells at a ratio of 20:1 (particles: cells) for 3 h. Data are expressed as the mean ± SD, n = 3, **p < 0.01, MP-NPs vs MPs at the same experimental conditions. Scale bar in (b, d) is 25 μm; scale bar in (c, e) is 10 μm.

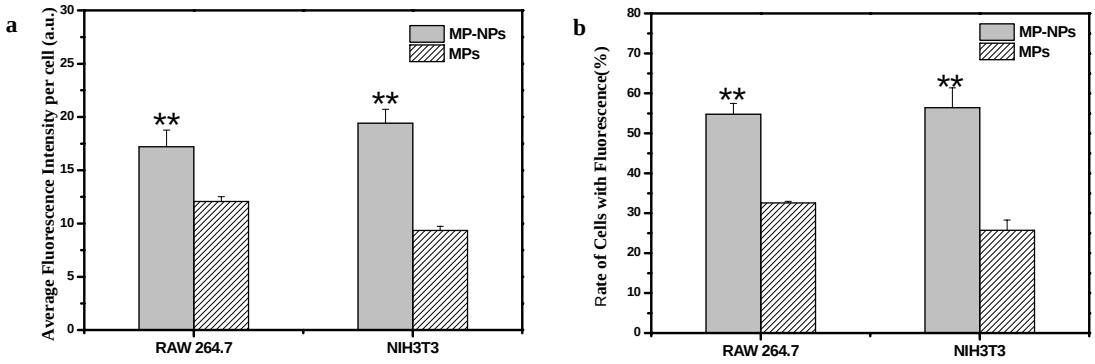

Figure S9 Flow cytometry results show the cellular uptake amount (a) and ratio (b) of MP-NPs and MPs by incubation with RAW 264.7 and NIH3T3 cells at a ratio of 20:1 (particles: cells) for 3 h, respectively. Data are expressed as the mean ± SD, n = 3, **p < 0.01, MP-NPs vs MPs at the same experimental conditions.

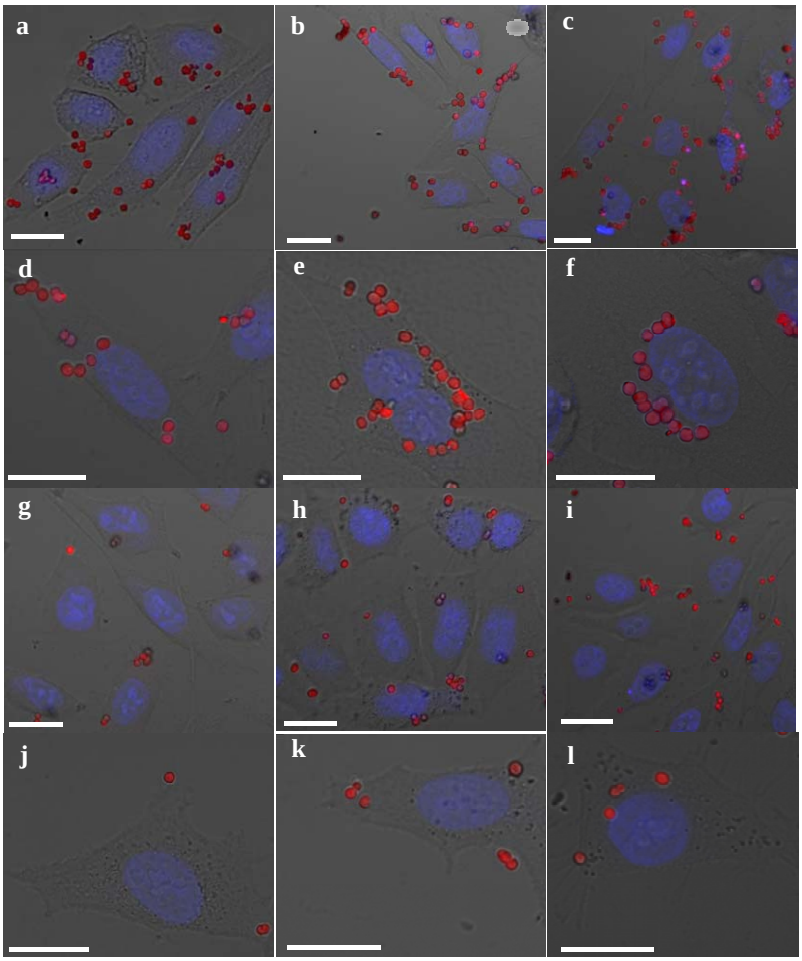

Figure S10 CLSM images show the cellular uptake of MP-NPs (a-f) and MPs (g-l) after being incubated with HepG2 cells at a particle-to-cell ratio of 20: 1 for 1 h (a, d, g, j), 3 h (b, e, h, k), and 6 h

(c, f, i, l), respectively. Scale bar: 20 μm.

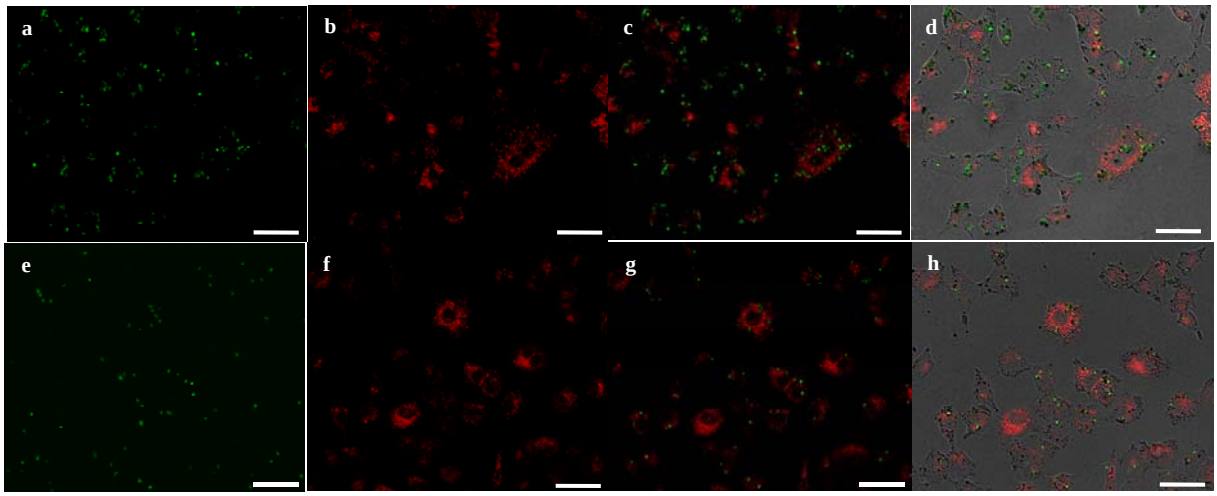

Figure S11 CLSM images of A549 cells after being incubated with MP-NPs (a-d) and MPs (e-h) at a particle-to-cell ratio of 20: 1 for 3 h. (a, e) Particles (green); (b, f) lysosomes (red); (c) and (g) merge images of (a) and (b), (e) and (f), respectively; (d) and (h) merge images of (c) and (g) with corresponding bright field channel images, respectively. Scale bar is 50 μm.

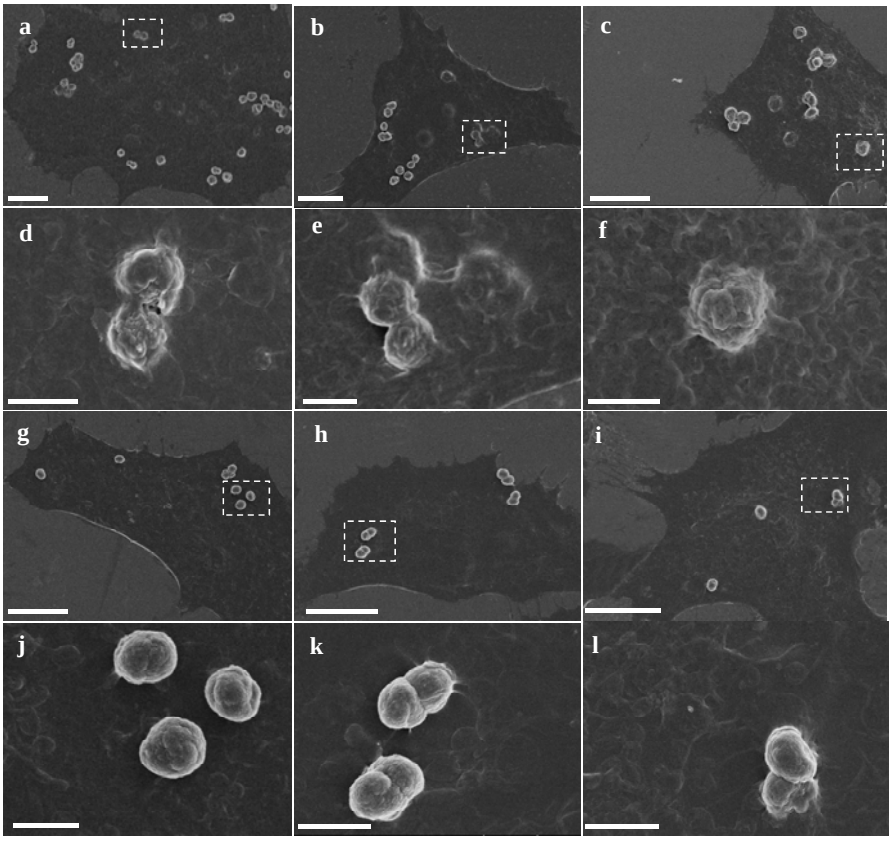

Figure S12 SEM images show the cellular uptake of MP-NPs (a-f) and MPs (g-l) after being

incubated with HepG2 cells at a particle-to-cell ratio of 20: 1 for 1 h (a, d, g, j), 3 h (b, e, h, k), and 6 h (c, f, i, l), respectively. (d), (e), (f), (j), (k) and (l) are the corresponding magnified SEM images of the rectangular areas in (a), (b), (c), (g), (h) and (i), respectively, showing details of the interaction between cells and particles. The samples were prepared by critical point drying. Scale bar in (a-c) and (g-i) is 10 μm; scale bar in (d-f) and (j-l) is 2 μm.

6. Intracellular ROS generation

In the PDT process, the activation of photosensitizers causes $^1O_2$ generation, raising oxidative stress. It should be noted that the DCFH-DA probe can detect various ROS and not singlet molecular oxygen. As mentioned in the text, under intracellular environment, DCFH-DA is deacetylated by esterases to obtain DCFH, and then DCFH is oxidized to the highly fluorescent DCF by various kinds of ROS. It is reported that peroxyl, alkoxyl, $NO_2^{\bullet}$, carbonate ($CO_3^{\bullet -}$), $OH^{\bullet}$ radicals as well as peroxynitrite can oxidize DCFH. However, H_2O_2 and $O_2^{\bullet -}$ can only oxidize DCFH in the presence of transition metal ions, peroxidases and heme proteins. [8-12]

The high level of intracellular ROS will inevitably do damage to the cells. As is shown in Figure S13, the cell morphology undertook distinct changes after being incubated with MP-NPs and light irradiation. Some cells became round, shrinking or even detached (Figure S13 a-d), which may indicate cell apoptosis. [13, 14] In contrast, for cells internalizing MPs, there were no obvious morphology changes after irradiation (Figure S13 e-h). By contrast, the control groups with light (Figure S14 b,f,j,n), MP-NPs (Figure S14 c,g,k,o) and MPs treatment only (Figure S14 d,h,l,p) showed fine cell morphology with negligible fluorescence compared with the cells only control (Figure S14 a,e,i,m), demonstrating no obvious ROS generation.

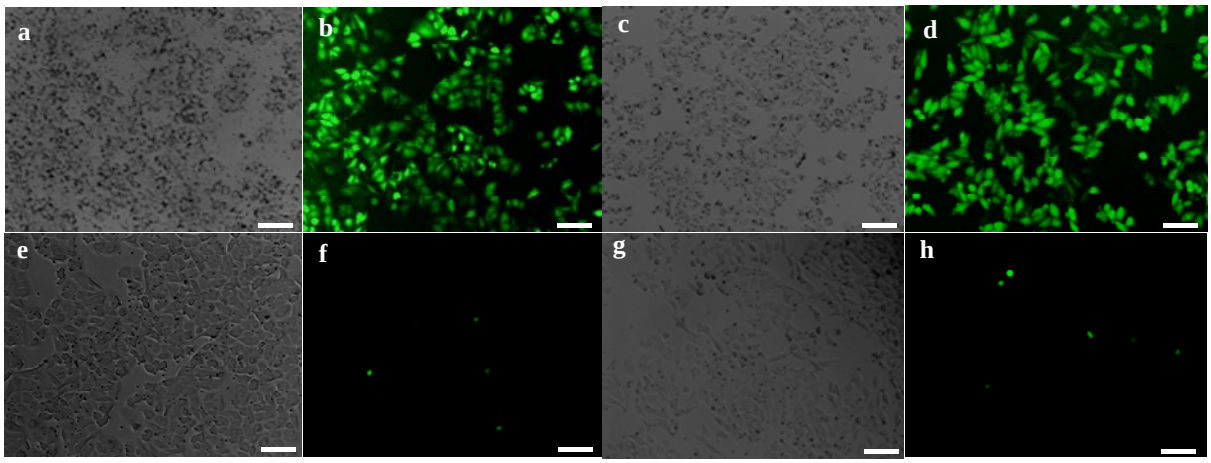

Figure S13 Transmission (a, c, e, g) and fluorescence (b, d, f, h) microscopy images show the production of reactive oxygen species (ROS) in A549 cells (a, b, e, f) and HepG2 cells (c, d, g, h) after being co-incubated with MP-NPs (a-d) and MPs (e-h) for 3 h, irradiated with a laser at 445 nm (0.3 W/cm^2, 5 s), and followed by incubation with DCFH-DA for 30 min. Scale bar is 100 μm.

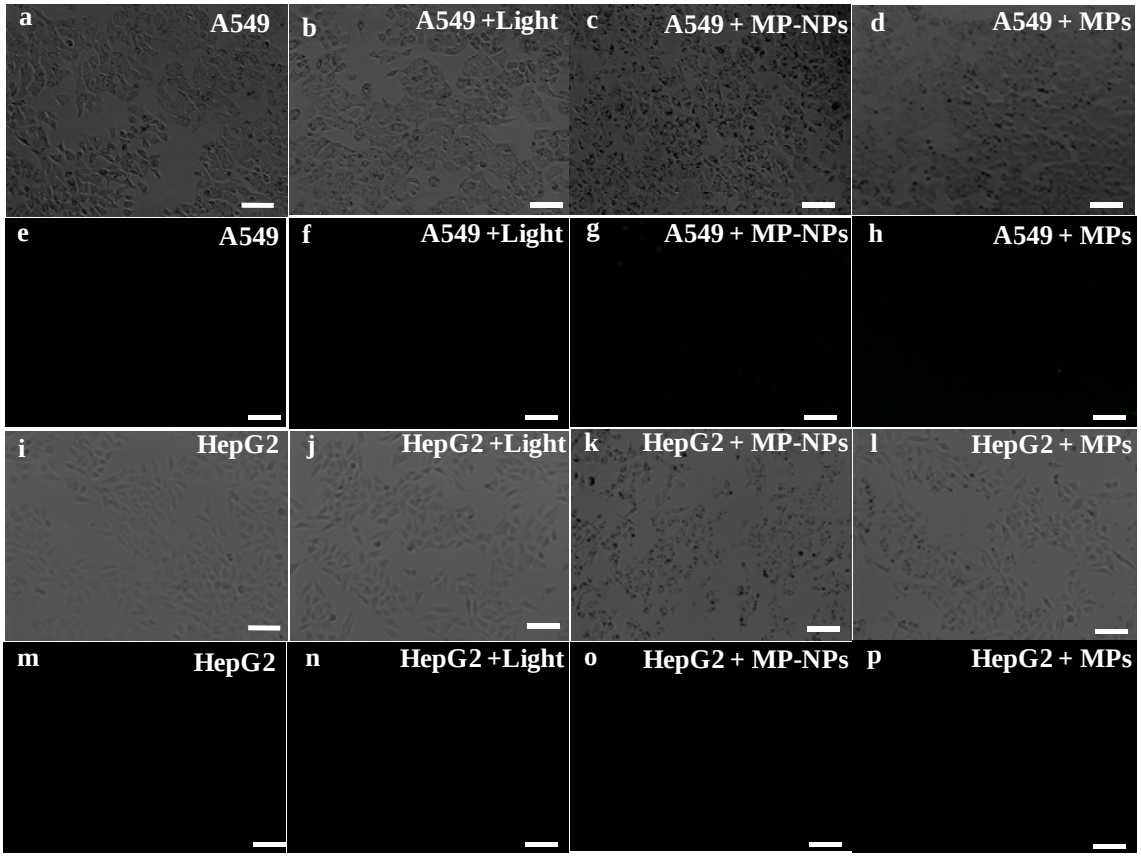

Figure S14 Transmission (a-d, i-l) and fluorescence (e-h, m-p) microscopy images show the regeneration of ROS in A549 cells (a-h) and HepG2 cells (i-p) without any treatment (a, e, i, m); being irradiated with a laser (0.3 W/cm^2, 5s) (b, f, j, n); and being co-incubated with MP-NPs (c, g, k, o) and

MPs (d, h, l, p) for 3 h (particles: cells = 20:1), respectively. The cells were incubated with DCFH-DA for 30 min after the above treatments. Scale bar is 100 μm.

7. PDT effect

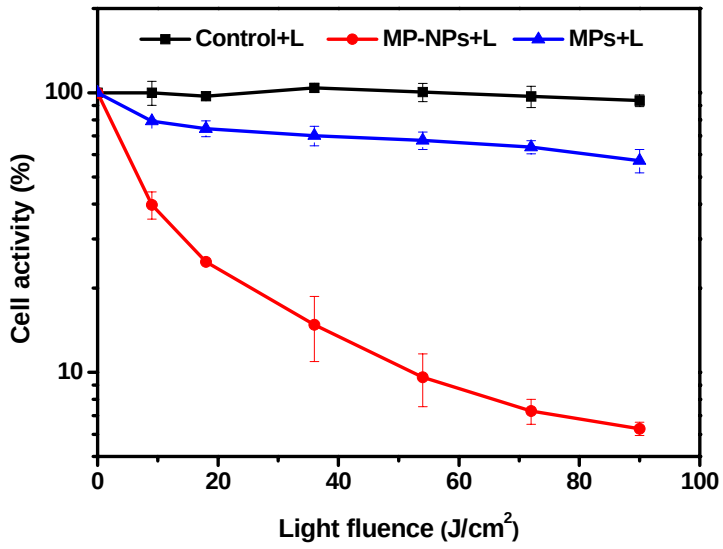

Figure S15 Light-dose response curves. Cytotoxicity of MP-NPs and MPs after co-incubation with A549 cells at a particle-to-cell ratio of 20:1 for 3 h, followed by irradiation with a laser at 445 nm (0.3 W/cm^2) for different light fluence values (9, 18, 36, 54, 72 and 90 J / cm^2), respectively. Data are expressed as the mean ± SD, n = 5.

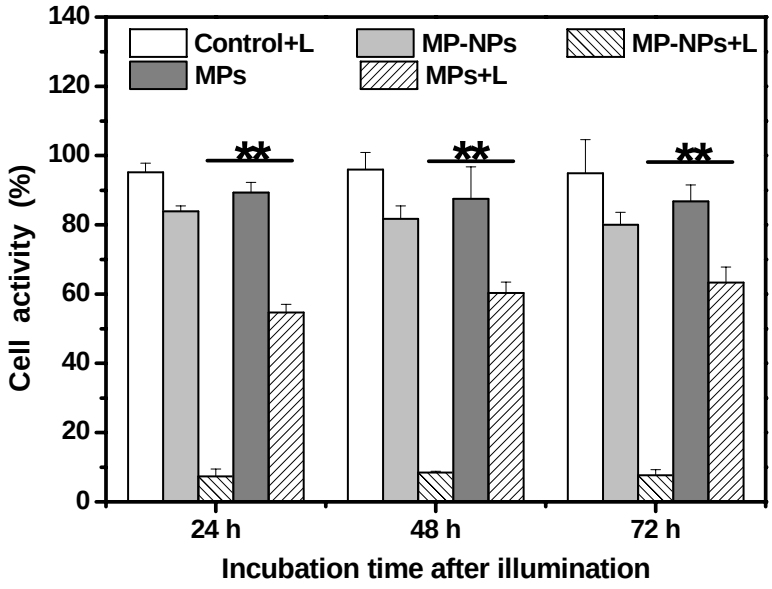

Figure S16 Long time PDT effect. Cytotoxicity of MP-NPs and MPs after co-incubation with

A549 cells at a particle-to-cell ratio of 20:1 for 3 h, followed by irradiation with or without a laser at 445 nm (0.3 W/cm^2, 5 min). After irradiation, the cells were further incubated for 24, 48 and 72 h and then tested with MTT assay, respectively. Data are expressed as the mean ± SD, n = 5, **p < 0.01, MP-NPs+L vs MPs+L at the same experimental conditions.

References

1 E. E. Bonfantini, A. K. Burrell, W. M. Campbell, M. J. Crossley, J. J. Gosperc, M. M. Hardingc, D. L. Officer and D. C. W. Reida, J. Porphyr. Phthalocya., 2002, 6, 708.

2 W. B. Zhang, L. B. Xing, H. S. Wang, X. J. Liu, Y. Q. Feng and C.Y. Gao, Langmuir, 2015, 31, 4330.

3 Z. P. Wang, H. Möhwald and C. Y. Gao, ACS Nano., 2011, 5, 3930.

4 C. F. van Nostrum, Adv. Drug Delivery Rev., 2004, 56, 9.

5 S. J. Lee, H. Koo, H. Y. Jeong, M. S. Huh, Y. Choi, S. Y. Jeong, Y. Byun, K. Choi, K. Kim and I. C. Kwon., J. Controlled Release., 2011, 152, 21.

6 K. Liu, R. R. Xing, C. J. Chen, G. Z. Shen, L. Y. Yan, Q. L. Zou, G. H. Ma, H. Möhwald and X. H. Yan., Angew. Chem. Int. Ed., 2015, 54, 500.

7 Y. J. Li, X. F. Li, Y. L. Li, H. B. Liu, S. Wang, H. Y. Gan, J. B. Li, N. Wang, X. R. He and D. B. Zhu, Angew. Chem., Int. Ed., 2006, 45, 3639.

8 H. Ischiropoulos, A. Gow, S. R. Thom, N. M. Kooy, J. A. Royall and J. P. Crow, Methods Enzymol., 1999, 301, 367.

9 P. Bilski, A. G. Belanger and C. F. Chignell, Free Radic. Biol. Med., 2002, 33, 938.

10 T. Ohashi, A. Mizutani, A. Mukarima, S. Kojo, T. Ishii and S. Taketani, FEBS Lett., 2002, 511, 21.

11 W. Jakubowski and G. Bartosz Cell Biol. Int., 2000, 24, 757.

12 M. Karlsson, T. Kurz, U. T. Brunk, S. E. Nilsson and C. I. Frennesson, Biochem. J., 2010, 428, 183.

13 A. Heidi and R. H. Michael, Biochem. J., 2016, 473, 347.

14 F. Hu, Y. Y. Huang, G. X. Zhang, R. Zhao, H. Yang and D. Q. Zhang, Anal. Chem, 2014, 86, 7987.